OPEN

Icosahedral AlCuFe quasicrystal at high pressure and temperature and its implications for the stability of icosahedrite

Vincenzo Stagno[1], Luca Bindi[2], Yuki Shibazaki[1], Yoshinori Tange[3,4], Yuji Higo[5], H.-K. Mao[1,6], Paul J. Steinhardt[7] & Yingwei Fei[1]

[1]Geophysical Laboratory, Carnegie Institution of Washington, Washington, DC 20015, USA, [2]Dipartimento di Scienze della Terra, Università di Firenze, Via La Pira 4, I-50121 Florence, Italy, [3]Geodynamic Research Center, Ehime University, Matsuyama, Japan, [4]Earth-Life Science Institute, Tokyo Institute of Technology, Tokyo 152-8550, Japan, [5]SPring-8, Japan Synchrotron Radiation Research Institute, Kouto, Hyogo 678-5198, Japan, [6]Center for High Pressure Science and Technology Advanced Research, Shanghai 201203, P. R. China, [7]Department of Physics and Princeton Center for Theoretical Science, Princeton University, Princeton, New Jersey 08544, USA.

The first natural-occurring quasicrystal, icosahedrite, was recently discovered in the Khatyrka meteorite, a new CV3 carbonaceous chondrite. Its finding raised fundamental questions regarding the effects of pressure and temperature on the kinetic and thermodynamic stability of the quasicrystal structure relative to possible isochemical crystalline or amorphous phases. Although several studies showed the stability at ambient temperature of synthetic icosahedral AlCuFe up to ~35 GPa, the simultaneous effect of temperature and pressure relevant for the formation of icosahedrite has been never investigated so far. Here we present *in situ* synchrotron X-ray diffraction experiments on synthetic icosahedral AlCuFe using multianvil device to explore possible temperature-induced phase transformations at pressures of 5 GPa and temperature up to 1773 K. Results show the structural stability of i-AlCuFe phase with a negligible effect of pressure on the volumetric thermal expansion properties. In addition, the structural analysis of the recovered sample excludes the transformation of AlCuFe quasicrystalline phase to possible approximant phases, which is in contrast with previous predictions at ambient pressure. Results from this study extend our knowledge on the stability of icosahedral AlCuFe at higher temperature and pressure than previously examined, and provide a new constraint on the stability of icosahedrite.

Quasicrystals[1,2], short for quasiperiodic crystals, are solids able to violate the conventional rules of crystallography because their structure is "quasiperiodic" rather than periodic; that is, their atomic density can be described by a finite sum of periodic functions with periods whose ratio is irrational. Their diffraction pattern consists of true Bragg peaks whose positions can be expressed as integer linear combinations of D integer linearly independent wavevectors where D is greater than the number of space dimensions. Among the quasicrystals made in the laboratory, many exhibit a three-dimensional icosahedral symmetry defined by $D = 6$ integer linearly independent wavevectors, a symmetry strictly forbidden for crystals. To date, quasicrystals (QC) have been widely studied because of their potential industrial applications, such as hydrogen storage, hydride battery materials and coating of soft metals[3]. The stability of i-QC structures with various compositions such as i-AlMn, i-AlCuRe or i-TiZrNi has been also investigated at high pressure and ambient temperature, in most cases based only on powder diffraction. The majority of studies are at pressures less than 40 GPa; only i-AlLiCu has exhibited a transformation to a crystalline phase within its measured pressure range. A review of high-pressure studies for various i-QC compositions has been compiled by Krauss and Steurer[4].

Among the several synthetic quasicrystalline solids, icosahedral-$Al_{63}Cu_{24}Fe_{13}$ is particularly fascinating as it is the composition of icosahedrite, the first natural-occurring quasicrystal[5,6]. An extraterrestrial origin has been recently established for icosahedrite[7,8], and its association with stishovite and other high pressure phases suggests formation at high pressures and temperatures during an impact-induced shock[9]. In the laboratory, the formation of synthetic i-AlCuFe was extensively investigated at ambient pressure[10-15]. These studies showed that the

formation and stability of i-AlCuFe depended sensitively on composition and temperature. In addition, several subsolidus phases that can coexist with the i-QC were described in the Al-Cu-Fe system. For instance, at ambient pressure the stability field of i-QC expands gradually as the Cu-Fe content increases from 24–12 to 26–13 atom% as the temperature increases from ~373 K to ~1123 K, beyond which the alloy melts incongruently to produce a liquid coexisting with a cubic and/or monoclinic crystalline phase. Above ~1273 K the system is predicted to be totally molten, at least at ambient pressure[10,16]. Studies of phase equilibria in the Al-Cu-Fe system by Zhang and Lück[11–15] are additional valuable contributions towards a full understanding of the solidification sequence in the vicinity of the quasicrystal region with respective subsolidus assemblages at ambient pressure.

Interestingly, in all these studies, neither a phase transformation to an ordered crystalline phases nor amorphization has been found so far in quasicrystals with composition $Al_{62}Cu_{25.5}Fe_{12.5}$, at ambient temperature, at least up to 35 GPa[17].

A few studies describe the synthesis and stability of i-QC at relatively low temperature (623–1113 K) and low pressure (uniaxial compression testing[18]) up to 1.64 GPa[19]. To date, though, there have not been the wider range of P-T conditions needed to get a fuller understanding of the stability of i-AlCuFe generally and, specifically, to gain a better understanding of the processes that account for the occurrence of icosahedrite in the Khatyrka meteorite. In particular, it is important to understand whether i-AlCuFe retains icosahedral symmetry at high pressure and temperature or easily transforms either into a periodic approximant[20,21] or other crystalline phase[16,22].

In this study we present the results of the first in situ synchrotron X-ray diffraction measurements of i-AlCuFe conducted at both high pressure and temperature. In addition, we present a (ex situ) single-crystal X-ray analysis of the recovered samples to investigate possible structural high P-T induced transformations. The results provide important insights on the stability of quasicrystals and the formation of icosahedrite.

Results

***In situ* diffraction measurements.** To understand the role of temperature on the stability of i-AlCuFe at high pressure, the i-AlCuFe starting material loaded in a graphite capsule was pressurized directly to a pressure of ~5 GPa at room temperature. In situ energy-dispersive X-ray diffraction patterns were then measured while increasing the temperature from 298 to 1673 K at constant press ram load of 3MN. The target pressure was determined from the equation of state of Au[23] and MgO[24] used as pressure markers which were placed at the top of the sample as a powder mixture. The unit-cell volume of Au (65.82 ± 0.01 Å^3) was calculated from the position of the 111, 200 and 220 peaks. The 111, 200 and 220 peaks of MgO were also used ($V = 72.51 \pm 0.14$ Å^3). The pressures determined from the two markers were 5.54 GPa and 5.08 GPa, respectively. Figure 1a shows the typical diffraction pattern of i-AlCuFe starting material measured at ambient conditions. Peaks are indexed as in Figure 2 using the Cahn indexing scheme[25] with interplanar distances being in agreement with those reported for natural icosahedrite[6]. Figure 1b shows diffraction patterns collected during heating at constant pressure in the energy range of 30–145 keV. Variations in the nominal pressure owing to the thermal expansion, however, are known and expected to be within 1–1.5 GPa[26]. For the purposes of this study, this small pressure shift can be considered negligible. The diffraction pattern of the sample measured after compression at room temperature shows broader diffraction peaks compared with that measured at ambient conditions (Figure 1a). We interpret this feature as arising from lattice strain effects during sintering of the starting powder. As temperature increases, the peaks become sharper similar to what has been observed during annealing or rapid quenching experiments of i-

QC[10], and explained as likely due to the increase in quasiperiodic translational order. The secondary phase ($AlFe_3$) found in the starting material was observed in situ to disappear at temperature >973 K as also observed by Turquier et al.[19]. Additional peaks are present in the collected diffraction patterns and are characteristic of the MgO and graphite from the surrounding sleeve and capsule material, respectively. Preferred orientation occurs during quenching as suggested by the increased intensities of few peaks at 60–80 keV energy range. Therefore, results from in situ high P-T energy dispersive diffraction measurements show that no additional peaks appear after recovering the sample at ambient conditions, but peaks that disappear are relative to the $AlFe_3$ phase initially present in the starting material. This would suggest that homogenization of the starting material occurred within the duration of our measurements, and demonstrate kinetic, and perhaps thermodynamic stability, of the i-AlCuFe quasicrystal over the entire temperature range investigated in this study.

Temperature dependence of the *d*-spacings. In situ energy-dispersive X-ray diffraction of specimens with wide d-spacing within a fixed energy interval was measured. We used a low angle (3.9775°) that made it possible to measure the thermal dependence of interplanar distances between 1.2 and 3.4 Å. The observed d-spacings were determined by fitting each peak using Gaussian + Lorentian functions and values are reported in Table 1 within an uncertainty of < 1%. The d-spacings decrease by 1.0–1.6% with respect to the initial values when pressure increases from ambient to 5 GPa. The temperature dependence of the observed d-spacing from 11 peaks is shown in Figure 2. No significant change occurs during heating aside from the d-spacing increasing linearly. More importantly, this confirms the structural stability of i-AlCuFe up to 1673 K. The structural anisotropy of i-AlCuFe can be observed in Figure 3, where the measured interplanar distances (d) are shown with respect to the initial d-spacing (d_0) and plotted as a function of temperature. No evident anisotropy is observed for the majority of the d-spacings, but a sharp change in the volumetric thermal expansivity is evident at ~1200 K. This can be explained as a result of the relaxation of the i-QC structure as the sample approaches the melting temperature. This also would agree with the peak sharpening observed in Figure 1b and with what has been observed by X-ray diffraction on rapidly quenched and annealed icosahedral phases, where the increase in temperature is accompanied by the relaxation of phason disorder and mark the proximity to the melting point and instability of i-QC. This temperature was estimated to be 1145 K (temperature at which the i-phase is totally molten) at ambient pressure, but it is at least 500 K higher at a pressure of 5 GPa.

The diffraction peaks were indexed using Cahn indices (N, M) which enable the determination of the six-dimensional lattice parameter, a_{6D}, following the scheme proposed by Steurer and Deloudi[27] (see also ref. 28),

$$a_{6D} = d\sqrt{\frac{N + M\tau}{2(2+\tau)}} \qquad (1)$$

where d is the d-spacing in Å, N and M the Cahn indices for which the d-spacing is experimentally determined, and τ is the golden ratio (($1 + \sqrt{5}$)/2). Calculations of a_{6D} at 298 K and 5 GPa gives 12.49 Å. This value is smaller than the value provided by Bindi et al.[6] for icosahedrite (12.64 Å) and reflects the pressure effect on the lattice parameter. In addition, our a_{6D} value at 5 GPa and room temperature is consistent with that predicted using both the equation of state by Sadoc et al.[17] and by Lefebvre et al[20]. In the first case, the pressure calculated using the a_{6D} from this study along with a fixed bulk modulus of 139 GPa and pressure derivative of 2.7 (Sadoc et al.[17]) is ~5.5 GPa. A pressure of 6 GPa is calculated using compressibility
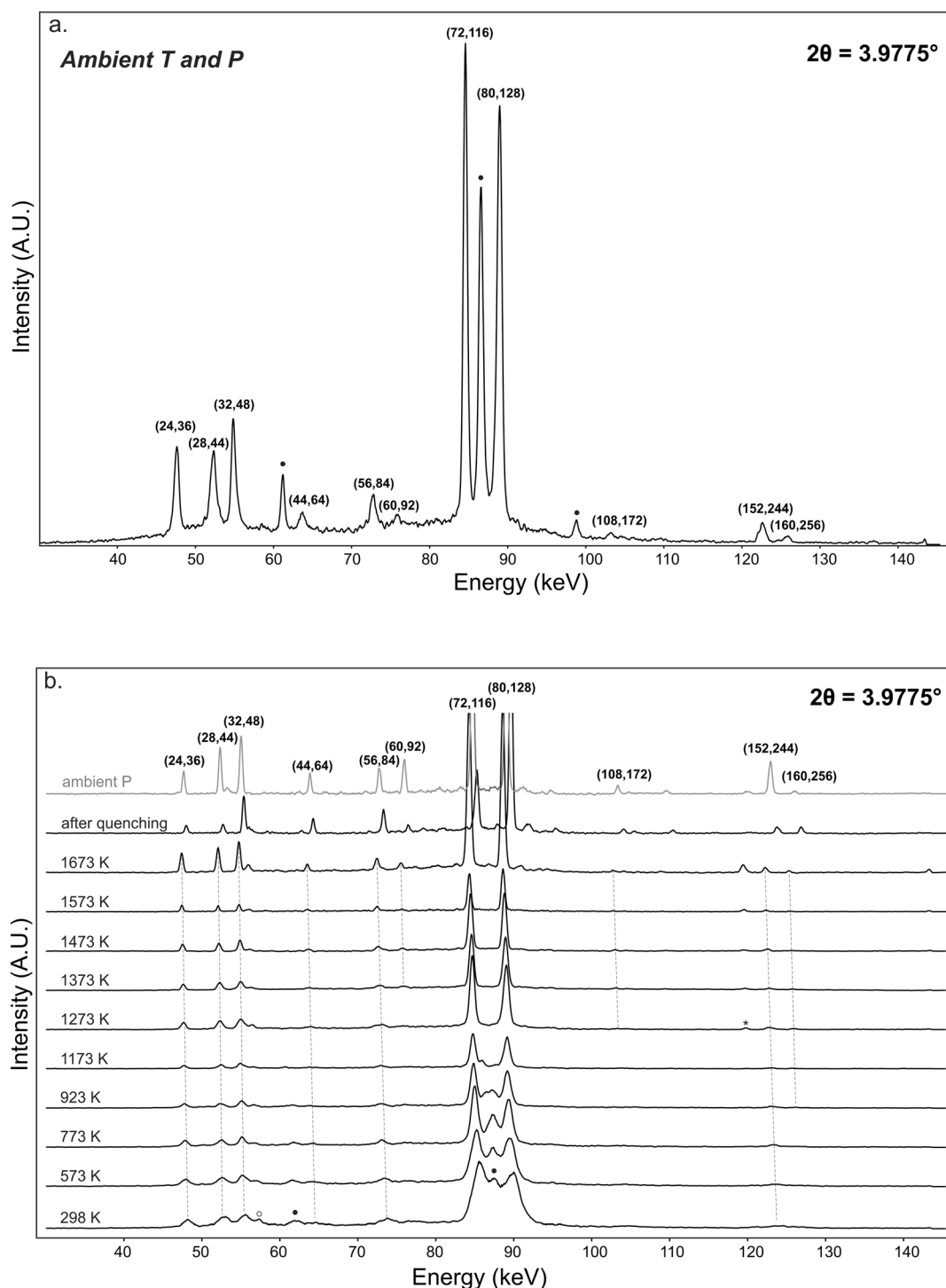
Figure 1 | (a) XRD pattern in energy-dispersive mode of i-QC starting material at ambient conditions. Filled circles indicate peaks representative of a secondary phase (AlFe₃) resulting from the synthesis procedure. (b) Temperature dependence of XRD patterns for i-QC. Notes: (*) MgO from surrounding sleeve; (˙) AlFe₃; (°) graphite peak from the surrounding capsule.

data by Lefebvre et al[20] (bulk modulus of 155 GPa and pressure derivative of 2).

A plot of the six-dimensional lattice constant with temperature is shown in Figure 4. This data can be fit using a second-order polynomial equation,

$$a_{6D} = a_{6D0} + \alpha T + \beta T^2 \qquad (2)$$

where $a_{6D0} = 12.49$ Å, T is the temperature in Kelvin, and α and β are the thermal expansion coefficients. Interestingly, we fit our data

using equation (2) with the values of α and β obtained by Quivy et al[29] for $Al_{62}Cu_{25.5}Fe_{12.5}$ (4.67×10^{-5} Å^{-1} K^{-1} and 5.22×10^{-8} Å^{-1} K^{-2}, respectively). The good fit indicates either that effects of chemical variations in the thermal expansion coefficients are small or that there is a negligible pressure effect on the volumetric expansion of icosahedrite. More generally, our results show that as pressure increases the structure of i-AlCuFe remains kinetically stable (and perhaps thermodynamically stable) at higher temperatures than previously investigated.
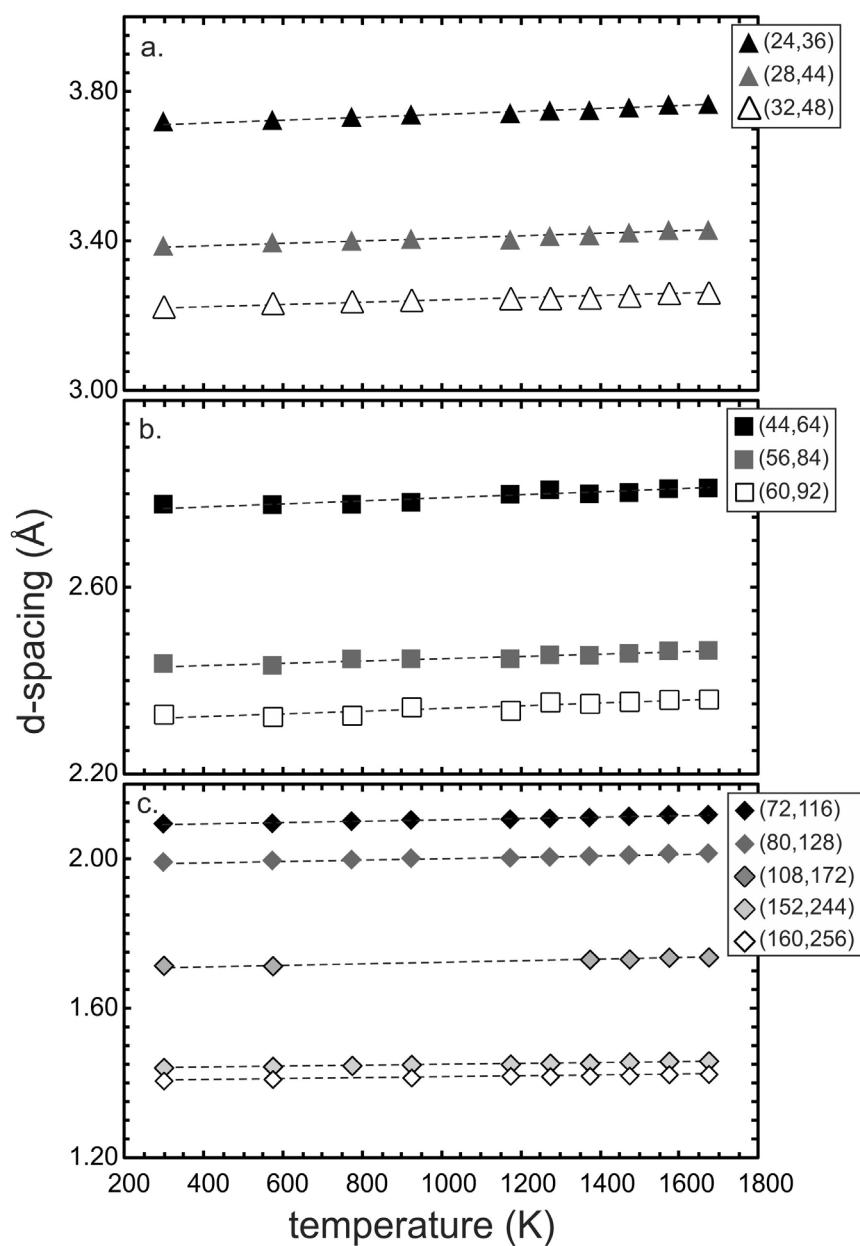
Figure 2 | Variation of *d*-spacings with temperature. Dashed lines are linear fits.

Table 1	Temperature dependence of interplanar distances at 5 GPa										
Run	T (K)	(24, 36)	(28, 44)	(32, 48)	(44, 64)	(56, 84)	(60, 92)	(72, 116)	(80, 128)	(108, 172)	(152, 244)	(160, 256)
ambient pressure	298	3.754	3.413	3.256	2.799	2.455	2.358	2.113	2.008	1.731	1.457	1.421
	298	3.710	3.378	3.210	2.762	2.419	2.308	2.087	1.990	1.711	1.437	-
	373	3.725	3.397	3.235	2.778	2.433	2.324	2.096	1.997	1.715	1.446	-
	773	3.734	3.402	3.239	2.778	2.447	2.327	2.102	1.999	-	1.448	-
	923	3.740	3.407	3.243	2.794	2.448	2.345	2.106	2.003	-	1.451	-
	1173	3.743	3.405	3.248	2.807	2.448	2.337	2.107	2.004	-	1.452	-
	1273	3.750	3.414	3.248	2.809	2.456	2.356	2.109	2.006	-	1.454	-
	1373	3.751	3.416	3.249	2.799	2.455	2.352	2.112	2.008	1.733	1.454	-
	1473	3.758	3.423	3.254	2.803	2.459	2.357	2.115	2.011	1.734	1.458	-
	1573	3.766	3.430	3.262	2.812	2.465	2.361	2.119	2.015	1.738	1.460	-
	1673	3.768	3.430	3.263	2.813	2.465	2.362	2.120	2.016	1.739	1.461	-
quenched	298	3.722	3.388	3.225	2.779	2.437	2.329	2.095	1.993	1.717	1.443	-
decompressed to ambient pressure	298	3.749	3.414	3.246	2.797	2.455	2.351	2.109	2.006	1.728	1.453	-

Figure 4 | Thermal dependence of the six-dimensional lattice parameter. Dashed line is a fit using equation (2).
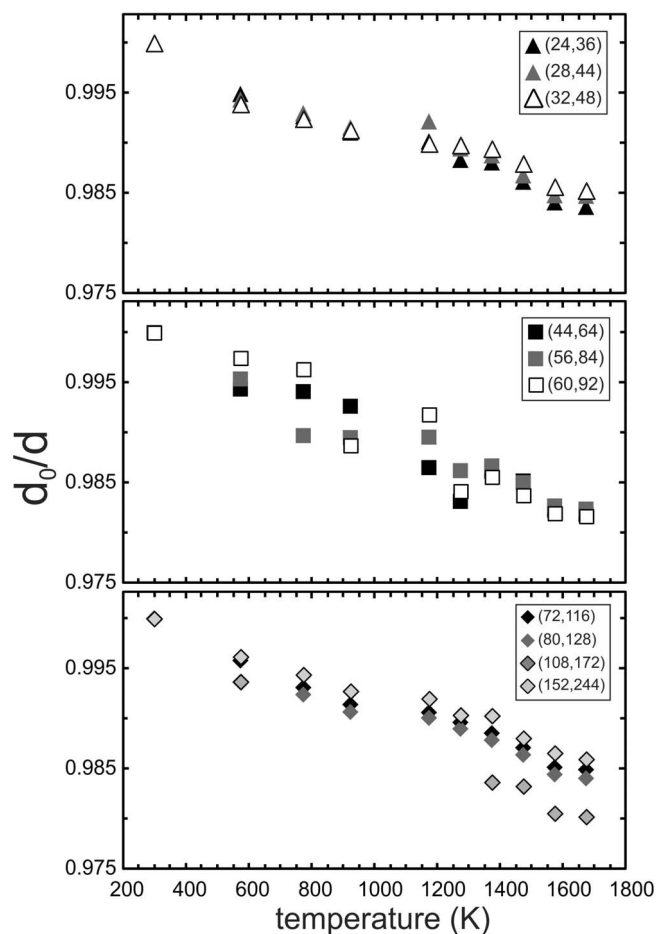
Figure 3 | Relative interplanar distances d_0/d as function of temperature. No evident anisotropy is observed during the thermal expansion of i-QC.

Analyses of the recovered samples. *Texture and Composition.* The recovered samples from both *in situ* and quench experiments consisted of hard metal chunks that were polished to investigate textural features and chemical composition. Figure 5a shows a sample recovered from 5 GPa and 1173 K with i-AlCuFe with nominal composition (±1 atomic% for Al and Cu) coexisting with minor amounts of cupalite (bright phase in Figure 5a). The grains appear still quite heterogeneous in size, but the combined effect of pressure and temperature resulted in the formation of dihedral angles along the grain boundaries. On geometric basis, considering that the cross section of an icosahedron is a pentagon or a decagon, we interpret this texture as evidence of a change in morphology of the initial spherical grains into faceted "soccer ball-like shapes" upon heating under pressure. The SEM image of a second sample quenched at the same pressure but at 1673 K is shown in Figure 5b. No secondary phase occurs, which indicates homogenization of the sample also consistent with the measured diffraction pattern from the same sample (Figure 1b). The chemical heterogeneity that can be inferred from the different brightness of the grains observed from the back-scattered electron image (Figure 5b) is also confirmed by compositional analyses where the Al content slightly decreases by ∼2 atom% with respect to the nominal composition. One possible reason for this chemical variation is the partial oxidation of i-AlCuFe during the experiments; however, small chemical heterogeneities in the industrially fabricated starting material cannot be excluded as also confirmed by chemical analyses of the starting quasicrystalline powder (see the Methods section). As mentioned above, the choice of a graphite capsule was to minimize oxidation during our experime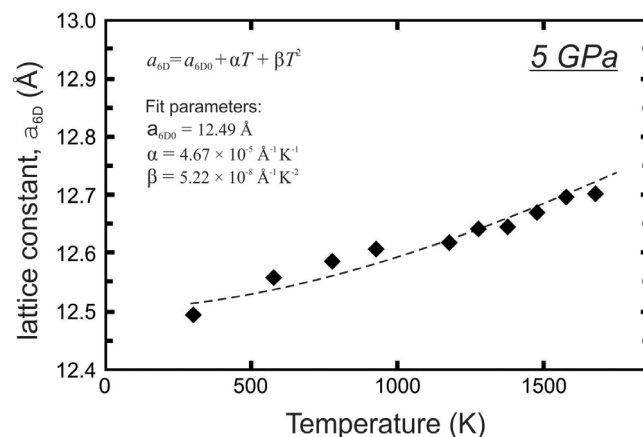nts. On the other hand, we cannot exclude possible oxidation of the starting material during the high-temperature treatment at high pressure, as it is known that graphite containers only would set an upper limit of fo_2 near the CCO buffer[30,31] by the reaction,

$$C + O_2 = CO_2 \qquad (3)$$

at which i-AlCuFe is expected to be unstable. The partial oxidation of i-AlCuFe, although not detected during *in situ* measurements, is confirmed by a very thin film with low brightness (low atomic number) surrounding some particles of the recovered sample (less significant in the sample quenched at 1173 K) from which we can only infer its oxygen-related composition (Figure 5b). Nevertheless, the formation of Al_2O_3 by oxidation of i-AlCuFe would be also supported by the free enthalpy of formation for Al_2O_3 compared to the oxidized Fe- and Cu-phases[32].

An additional quench experiment was performed at a similar pressure (5 GPa) and 1773 K for 30 min to investigate possible decomposition reactions or melting of the i-AlCuFe phase. To this end, we used the same capsule and starting material as for the *in situ* X-ray diffraction measurements. Results are shown in Figure 5c. It can be seen that multiple phases occur in the Al-Cu-Fe system coexisting with randomly elongated Al needles. Corundum was also found in minor amounts and likely formed after partial oxidation. In any case the coexistence of small amounts of Al and Al_2O_3 would be an indication that negligible amounts of oxygen were involved in chemical reactions. The main phases consist of Al-Cu-Fe solid solutions with different stoichiometry coexisting with a melt.

For a clear identification and visualization of these Al-bearing phases, high-resolution chemical maps were collected over a 12 hr exposure time; an example of the results processed is shown in Figure 6. The two identified solid phases have the following average chemical composition 1) 45.19(±0.63) wt% Al, 33.69(±0.66) wt% Cu and 21.95(±0.66) wt% Fe and 2) 28.58(±1.05) wt% Al, 64.03(±0.84) wt% Cu and 7.72(±1.05) wt% Fe. On the basis of normalized total atoms (to 100) these phases can be written with the formula $Al_{64.55}Cu_{20.21}Fe_{15.24}$ and $Al_{48.03}Cu_{45.70}Fe_{6.27}$ (Al/Cu ∼1:1). These phases correspond to the β-phase (unknown phase in nature) and Fe-bearing CuAl (natural Fe-rich cupalite). Figure 5c shows also the presence of minor amounts of melt with composition 33.59(±0.19) wt% Al, 40.52(±0.44) wt% Cu and 25.50(±0.66) wt% Fe. We conclude that i-AlCuFe is thermodynamically unstable at $T > 1673$ K, and decomposition occurs in short time (within 30 min) to form two solid phases + liquid in the Al-Cu-Fe system. It is not clear whether Al is also a product of the decomposition or forms directly from the melt during quenching. Textural observations support the latter.
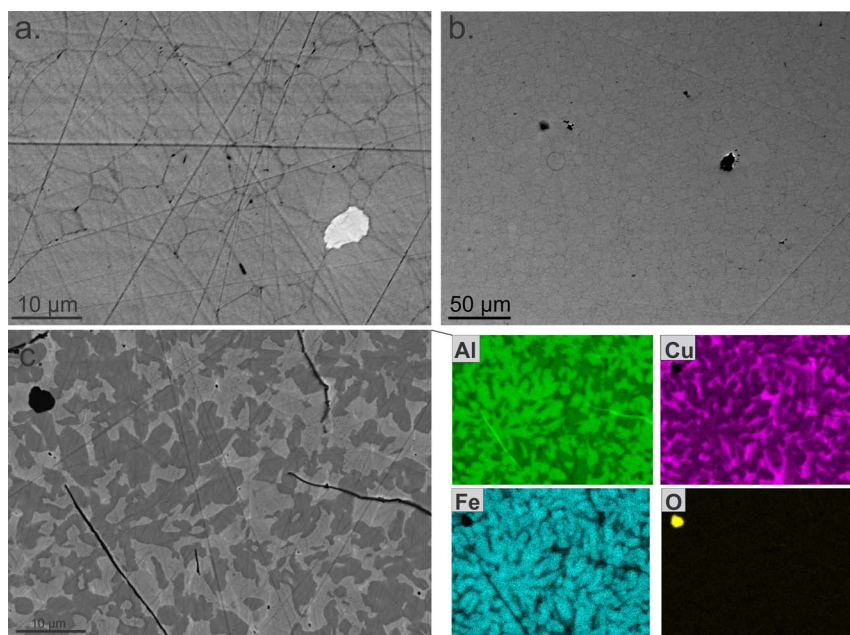
Figure 5 | Back-scattered electron (BSE) images obtained using a scanning electron microscope (SEM) of the recovered sample from runs at 5 GPa and 1173 K (a) and 1673 K (b), respectively. c) SEM-BSE image of the run at 5 GPa and 1773 K with relative X-ray compositional maps for Al, Cu, Fe and O.

Ex situ X-ray diffraction measurements. As stated above, the *in situ* X-ray diffraction patterns (Figure 1a–b) were indexed following Bindi et al.[6]. The observed linear increase of *d*-spacings with temperature, as well as the absence of significant anisotropy during thermal expansion are evidence of the stability of i-AlCuFe at high pressure within the duration of our experiments. Further, the thermal expansion coefficients obtained from the fits are consistent with those discussed above reported by Quivy et al.[29] from ambient pressure measurements and show the large kinetic stability. However, it should be noted that approximant phases might form as the icosahedrally symmetric phase is unstable. The subtle transformation from aperiodic to periodic structures has been widely debated in literature[33]. This implies that extreme prudence must be taken in order to identify the phases found in samples recovered after being quenched from extreme conditions. Figure 7a is a powder diffraction pattern (Cu*K*α radiation) of the sample recovered from 5 GPa and 1673 K and for which indexing of the peaks in agreement with the diffraction pattern of the natural i-AlCuFe, icosahedrite, is possible. However, it can be seen that new reflections with low intensity

appeared in the 2θ range between ∼38 and 50°. These peaks were also observed during *in situ* measurements immediately after quenching and at ambient pressure (see Figure 1). We note that the formation of approximant phases from i-AlCuFe phase was previously described by Bancel[10], who claimed in his case that the changes in the diffraction pattern caused by annealing are due to the transformation to a crystalline structure. Therefore, in order to determine if the phase quenched from these high *P-T* conditions retained its icosahedral symmetry, single-crystal X-ray diffraction measurements were performed on a micrometer grain taken from the sample in the experimental capsule. The result is shown in Figure 7b where a reconstructed precession image down the five-fold symmetry axis obtained using all the collected reflections shows unequivocally that the icosahedral symmetry is retained on recovery from high *P-T* conditions. Notably, no split of reflections was observed, thus excluding the possibility that the five-fold symmetry is simulated by twinning of high-temperature approximants. The reflections characterized by low intensity in Figure 7a appear as consequence of preferred orientation (or grain growth) induced by the high temperature involved in the experiments, and can be considered characteristic of i-AlCuFe, rather than evidence of the transformation to crystal observed by Bancel[10]. Hence, these measurements confirm that the material considered here is i-AlCuFe, the analogue of the natural quasicrystal icosahedrite.

Discussion

This study represents the first extensive experimental investigation of the stability of the i-AlCuFe quasicrystal structure at high *P-T*. Previous *in situ* diffraction measurements studies at ambient temperature revealed that the stability of the quasicrystal phase can persist up to ∼35 GPa[17,34]. For comparison, the amorphization of the quasicrystal phase i-AlLiCu was observed to occur just above 10 GPa with a transition to a crystalline structure occurring above 28 GPa[35]. The results of the present study clearly show that i-AlCuFe remains in its i-QC structure up to 5 GPa and 1673 K within the duration of our experiments.

Previous work by Bancel[10] at ambient pressure and lower temperature (848 K) showed that the i-QC only formed in a narrowing
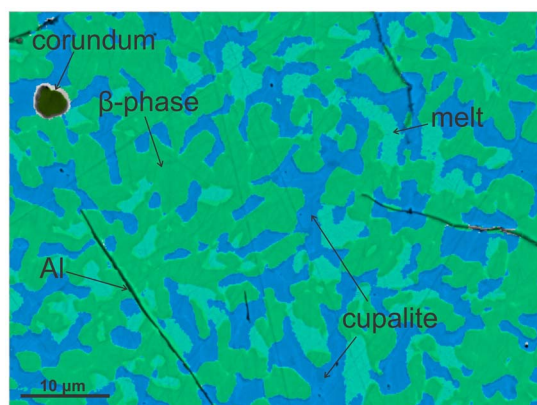

Figure 6 | High-resolution image obtained after compositional mapping showing the spatial distribution of the recovered phases in the Al-Cu-Fe system.
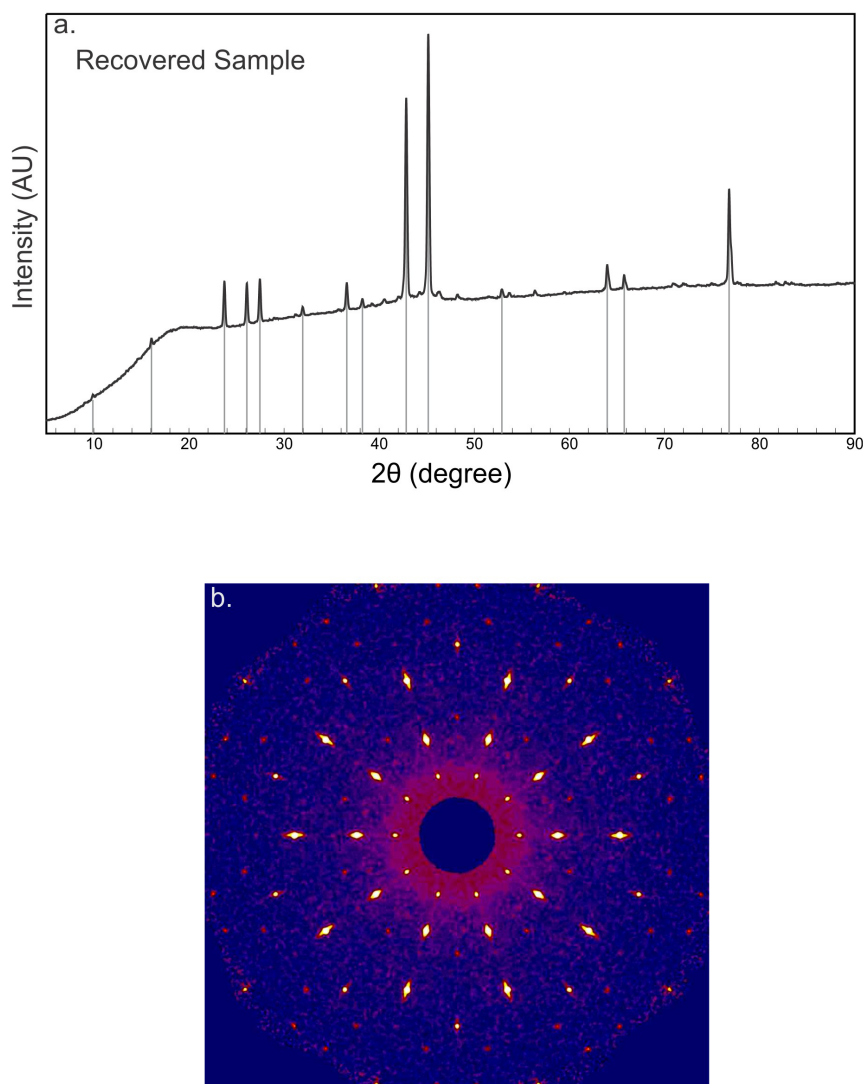
Figure 7 | X-ray powder diffraction pattern (Cu$K\alpha$ radiation) of the sample recovered from 5 GPa and 1673 K (a). Grey lines are used to mark peaks representative of i-AlCuFe that can be indexed according to Bindi et al.[6] (see also Figure S1b). b) A reconstructed precession image down the five-fold symmetry axis obtained using the collected single-crystal X-ray reflections from a fragment of the same sample as in (a) compatible with icosahedral symmetry.

compositional range as temperature decreased. Bancel also noted changes in the diffraction pattern under annealing due to the transformation to a crystalline structure. By contrast, no indication of a transformation to a crystalline phase was found in this high-pressure study at substantially high temperatures (up to 1673 K). Furthermore, it is notable that, starting from a QC with composition of Al$_{63}$Cu$_{24}$Fe$_{13}$, our high pressure experiments at T of 1773 K show the presence of a liquid phase coexisting with two solids (β-phase and cupalite). It is, therefore, expected that if congruent melting of i-AlCuFe occurs, this can only happen between 1673 K and 1773 K before the i-QC decomposes. In contrast, Bancel observed a coexisting λ-phase (Al$_{13}$Fe$_4$) at ambient pressure up to 1073 K in the same Al-Cu-Fe compositional region. These observations are evidence that higher pressure acts to stabilize i-AlCuFe at higher temperature, and that, prior to complete melting of the i-Al$_{63}$Cu$_{24}$Fe$_{13}$, decomposition occurs with two coexisting solid phases (β-phase and cupalite) along a cotectic. The absence of the λ-phase (Al$_{13}$Fe$_4$) both in the in situ energy-dispersive X-ray diffraction patterns and the recovered samples would raise important questions about its stability at high P and T.

The high P-T studies of synthetic i-AlCuFe are of special interest because the materials have the same composition as icosahedrite, the first natural quasicrystal[5,6]. Icosahedrite was found in grains of the Khatyrka meteorite, a CV3 carbonaceous chondrite[8]. The icosahedrite in the meteoritic grains was closely associated with minerals such as spinel, diopside, forsterite, nepheline, sodalite, corundum, stishovite, khatyrkite (CuAl$_2$), cupalite (CuAl), and an unnamed phase of composition AlCuFe[5–8].

The bulk composition in the meteorite probably has an excess of Al and Cu compared to our laboratory sample, which has the bulk composition of i-AlCuFe. This may explain why the laboratory samples do not contain khatyrkite. Interestingly, our laboratory experiments show that cupalite equilibrated with β-phase and Al-Cu-Fe melt contains some Fe ($\sim$8 wt%), while cupalite coexisting with icosahedrite in the CV3 chondrite appears Fe-free, probably due to element partitioning with the coexisting silicates (e.g. olivine) at high temperature.

The presence of stishovite and other high-pressure phases reported in Khatyrka fragments[9] indicate that the meteorite underwent high-pressure metamorphism due to a shock induced by a hypervelocity impact with pressures exceeding 10 GPa and temperatures up to 1500 K. The impact occurred about 4.5 Gya in the early solar nebula, and the meteorite landed on Earth about 15 kya. From this we can conclude that icosahedrite is kinetically stable for 4.5 Gy

at ambient pressures and temperatures in space and, for 15 ky, kinetically stable under the ambient pressures and temperatures on Earth. The exposure of the meteorite to high pressure conditions was for a very short time compared to our laboratory study. Our studies are also consistent with the possibility that icosahedrite is thermodynamically stable at 5 GPa and temperatures up to 1673 K.

Our laboratory studies complement and help to explain the formation of icosahedrite because they demonstrate under controlled conditions that high pressures significantly enhance the kinetic stability of the quasicrystal phase even when it is exposed to high pressure for a much longer time than that occurred in space during the impact between extraterrestrial bodies.

It was also claimed that during the impact shock, heterogeneous pressure distributions are generated with portions that might have reached at least 5 GPa and 1473 K, where icosahedrite can be stable. Our experiments would set an upper limit for the stability of icosahedrite within this pressure regime taken into consideration that a fast cooling rate, consistent with our laboratory quench experiments, has been proposed during which icosahedrite might have formed.

At the same time, the occurrence of metallic aluminum in icosahedrite indicates extremely reducing conditions that are not yet understood. Also, explaining the chemistry that led to the association of Al with Cu in icosahedrite is a puzzle. Further insight could be provided by further laboratory high-pressure and possibly shock-wave experiments.

Methods

Starting material. The starting material used in this study is a synthetic icosahedral AlCuFe ($\geq$99.9%) quasicrystalline powder with variable grain size $\leq$ 25 μm (see Figure *S*1a) provided by Sigma-Aldrich (prod. n. 757934). The nominal composition is $Al_{65}Cu_{23}Fe_{12}$, and to the aim of this study it can be considered as the synthetic analogue of icosahedrite ($Al_{63}Cu_{24}Fe_{13}$). The use of a starting material which has the composition and structure of interest allowed us to avoid possible issues regarding the synthesis of QC, such as slow element diffusion and nucleation rate.

Quench experiments. A quench experiment was performed at 5 GPa using a 1500-ton Kawai-type press available at the Geophysical Laboratory, Carnegie Institution of Washington. Tungsten carbide anvils of 11 mm truncation edge length (TEL) were used with 18 mm edge length cast octahedra (Aremco Ceramacast) as pressure media. A graphite capsule was used and placed in the central portion of a cylindrical straight graphite furnace, surrounded by MgO sleeve and spacers. A ZrO_2 sleeve was used as thermal insulator outside the graphite heater. Graphite as capsule material was chosen to minimize possible oxidation of the i-QC. Commonly employed metal capsules such as Re, Fe, Mo or Pt might manifest chemical affinity with our starting material. To our knowledge, no reactions are reported in literature between carbon and quasicrystals. Pressure calibration of the employed assembly was performed using the phase transitions of quartz to coesite, $CaGeO_3$-garnet to perovskite, coesite to stishovite and olivine to wadsleyite[36]. The temperature during the experiments was monitored with a W-5%Re/W-26%Re (C-type) thermocouple inserted within an alumina sleeve, with the junction in contact with the top of the capsule. The sample was compressed to the target pressure at a rate of ~0.5 GPa/hr, then heated to a temperature of 1773 K and kept manually constant within $\pm$5 K for a period of 30 minutes. The sample was quenched by turning off the power to the furnace and, then, decompressed to ambient pressure.

Scanning electron microscopy and electron microprobe. The chemical composition of selected fragments of the starting material was obtained using a JEOL JXA-8600 electron microprobe operating at 15 kV accelerating voltage and 20 nA beam current (and a 1 μm beam diameter), with 30 s as counting time. Replicate analyses of synthetic $Al_{63}Fe_{24}Cu_{13}$ quasicrystal were used to check accuracy and precision. The standards were: metal-Al (Al), metal-Cu (Cu), and synthetic FeS (Fe). Results from four point analyses gave the following chemical formula $Al_{63.26(\pm1.18)}Cu_{23.82(\pm0.87)}Fe_{12.92(\pm0.56)}$, which is consistent with the composition of icosahedrite, the natural quasicrystal.

After the X-ray diffraction measurements, all the recovered samples were mounted in epoxy resin and polished parallel to the axial furnace direction for textural observation and chemical composition mapping by Field Emission Scanning Electron Microscope (FE-SEM; JEOL JSM 6500F). In the case of quantitative analyses using energy-dispersive X-ray spectroscopy, we performed the calibration at 15 kV and 1.1 nA employing metals (Fe, Cu, Al,) and oxides (Al_2O_3) as standards.

Powder and single-crystal X-ray diffraction. Phase identification on the recovered samples was performed by powder X-ray diffraction using a Bruker 2D-Phaser diffractometer and a Bruker D8-Discover (Cu$K\alpha$ radiation). Peaks from the quenched phases were then interpreted using Jade 6.0 software and relative PDF data

files used as reference patterns. X-ray analysis of the starting material is shown in the Supplemental Materials. The majority of the peaks can be indexed on the basis of six integer indices conventionally used for quasicrystals[5,6,27,37]. Additional peaks are due to small amounts of $AlFe_3$ (reference JCPDS 050-0955) likely resulting from the procedure used to synthesize the quasicrystalline powder[38].

Additional diffraction data on both the starting material and fragments of material from the experimental capsules (after the high *P-T* experiments) were collected using an Oxford Diffraction Xcalibur PX Ultra single-crystal diffractometer fitted with a 165 mm diagonal Onyx CCD detector (Cu$K\alpha$ radiation). The crystal-to-detector distance was 7 cm. Data were processed using the *CrysAlis* software package version 1.171.31.2 (Oxford diffraction[39]) running on the Xcalibur PX control PC. Figure *S*2 shows the collected reflections down the five-fold axis on a selected untreated fragment from the starting material. An excellent agreement with a diffraction pattern along the 5-fold axis of an icosahedral material can be observed.

***In situ* X-ray diffraction experiments at high pressure and temperature.** The experiments were performed at BL04B1 sector at SPring-8, JASRI (Japan), using the large-volume press Speed-Mk. II[40] with tungsten carbide cubes (11 mm truncation) as second-stage anvils and pyrophillite gaskets. ZrO_2 octahedra (18 mm edge length) were used as pressure media with MgO rods positioned along the X-ray path. The starting material used for the *in situ* diffraction measurements is the synthetic AlCuFe compound described above, loaded in a graphite capsule enclosed in a MgO sleeve with MgO spacers at the bottom and top. A mixture of MgO and Au was placed at the top of the capsule as pressure calibrants and separated from the sample by a rhenium (25 μm thick) and a graphite disk, respectively. This configuration allowed an immediate identification of the sample by radiographic images (Figure *S*3). Cylindrical graphite furnaces were used to heat the sample. Temperatures were measured using a C-type thermocouple connected to a rhenium disk at the top of a capsule placed at the center of the furnace. *In situ* energy-dispersive X-ray diffraction measurements were conducted using white X-rays up to 160 keV collimated to a 0.10 mm (vertical) by 0.05 mm (horizontal). A Ge solid-state detector was used for collecting diffraction patterns in energy dispersive mode. The Bragg angle was set using a horizontal goniometer[41]. Energy and diffraction angles were calibrated before the measurements using known energy values of characteristic X-rays of several metal standards (Cu, Mo, Ag, Ta, Pt, Au and Pb) and known lattice parameters of gold. *In situ* diffraction measurements for this study were performed mostly at a fixed low Bragg angle (2θ = 3.9775°) to investigate the behavior of the i-QC phase within a unique wide range of *d*-spacings between 1.23 and 5 Å that allowed the indexing of 11 reflections of the 14 known for icosahedrite[6]. Since no phase transformation has been shown for i-AlCuFe of similar composition up to 35 GPa[17], sample was pressurized directly to the target pressure and heated. Diffraction patterns were collected with an exposure time of 300 s. This time is certainly shorter compared to the typical annealing times of intermetallic compounds. Although several researchers have pointed out that the sluggish kinetics of the i-AlCuFe phase at high temperature result in long equilibration times, Kang and Dubois[18] first and then Turquier et al.[19] reported no appreciable time-dependent change in the positions of the X-ray reflections after annealing at different temperatures at both ambient pressure and 0.45 GPa. An oscillation system was used in which the stage of the multianvil press can rotate around the center of the pressure medium while collecting X-ray diffraction patterns. In such a way we were able to minimize the grain growth and preferred orientation effects on the diffraction peaks. The positions of the diffracted lines and refinement of Au and MgO pressure markers were performed using the PDIndexer software[42], while conversion of the diffraction peaks to *d*-spacing was done using the commercial software PeakFit.

1. Levine, D. & Steinhardt, P. J. Quasicrystals: A new class of ordered structures. *Phys. Rev. Lett.* **53**, 2477–2480 (1984).
2. Shechtman, D., Blech, I., Gratias, D. & Cahn, J. Metallic phase with long-range orientational order and no translational symmetry. *Phys. Rev. Lett.* **53**, 1951–1954 (1984).
3. Dubois, J. M. New prospects from potential applications of quasicrystalline materials. *Mat. Sci. Engin.* **A294–296**, 4–9 (2000).
4. Krauss, G. & Steurer, W. Why study quasicrystals at high pressures? in *High-Pressure Crystallography,* eds. Katrusiak, A., McMillan, P.F., 521–526 (2004).
5. Bindi, L., Steinhardt, P. J., Yao, N. & Lu, P. J. Natural Quasicrystals. *Science* **324**, 1306–1309 (2009).
6. Bindi, L., Steinhardt, P. J., Yao, N. & Lu, P. J. Icosahedrite, $Al_{63}Cu_{24}Fe_{13}$, the first natural quasicrystal. *Am. Mineral.* **96**, 928–931 (2011).
7. Bindi, L. et al. Evidence for the extraterrestrial origin of a natural quasicrystal. *Proc. Nat Acad. Sci.* **109**, 1396–1401 (2012).
8. MacPherson, G. J. et al. Khatyrka, a new CV3 find from the Koryak Mountains, Eastern Russia. *Met. Planet. Sci.* **48**, 1499–1514 (2013).
9. Hollister, L. S. et al. Impact-induced shock and the formation of natural quasicrystals in the early solar system. *Nat. Commun.* **5**, 1–8, doi:10.1038/ncomms5040 (2014).
10. Bancel, P. A. Order and disorder in icosahedral alloys. Quasicrystals. In: Series on Directions in Condensed Matter Physics, *World Scientific*, Edited by DiVincenzo, D.P. & Steinhardt, P.J. **16**, 17–55 (1999).
11. Zhang, L. & Lück, R. Phase diagram of the Al-Cu-Fe quasicrystal-forming alloy system. I. Liquidus surface and phase equilibria with liquid. *Z. Metallkd.* **94**, 91–97 (2003).

12. Zhang, L. & Lück, R. Phase diagram of the Al–Cu–Fe quasicrystal-forming alloy system. II. Liquidus surface and phase equilibria with liquid. *Z. Metallkd.* **94**, 98–107 (2003).

13. Zhang, L. & Lück, R. Phase diagram of the Al–Cu–Fe quasicrystal-forming alloy system. III. Liquidus surface and phase equilibria with liquid. *Z. Metallkd.* **94**, 108–115 (2003).

14. Zhang, L. & Lück, R. Phase diagram of the Al–Cu–Fe quasicrystal-forming alloy system. IV. Liquidus surface and phase equilibria with liquid. *Z. Metallkd.* **94**, 341–344 (2003).

15. Zhang, L. & Lück, R. Phase diagram of the Al-Cu-Fe quasicrystal-forming alloy system. V. Solidification behavior of Al-Cu-Fe quasicrystal forming alloys. *Z. Metallkd.* **94**, 774–781 (2003).

16. Gratias, D. *et al.* The phase diagram and structures of the ternary AlCuFe system in the vicinity of the icosahedral region. *J. Non-Cryst. Sol.* **153-154**, 482–488 (1993).

17. Sadoc, A. *et al.* X-ray absorption and diffraction spectroscopy of icosahedral Al-Cu-Fe quasicrystals under high pressure. *Phil. Mag.* **70**, 855–866 (1994).

18. Kang, S. S. & Dubois, J. M. Pressure-induced phase transitions in quasicrystals and related compounds. *Europhys. Lett.* **18**, 45–51 (1992).

19. Turquier, F. *et al.* Formation and stability of single-phase Al-Cu-Fe quasicrystals under pressure. *Rev. Adv. Mat. Sci.* **8**, 147–151 (2004).

20. Lefebvre, S. *et al.* Stability of icosahedral Al-Cu-Fe and two approximant phases under high pressure up to 35 GPa. *Phil. Mag.* **B72**, 101–113 (1995).

21. Quiquandon, M. *et al.* Quasicrystal and approximant structures in the Al-Cu-Fe system. *J. Phys. Cond Matter* **8**, 2487–2512 (1996).

22. Barbier, J.-N., Tamura, N. & Verger-Gaugry, J.-L. Monoclinic $Al_{13}Fe_4$ approximant phase: a link between icosahedral and decagonal phases. *J. Non-Cryst. Sol.* **153–154**, 126–131 (1993).

23. Fei, Y. *et al.* Toward an internally consistent pressure scale. *Proc. Natl. Acad. Sci. USA* **104**, 9182–9186 (2007).

24. Jackson, I. & Rigden, S. M. Analysis of *P-V-T* data: Constraints on the thermoelastic properties of high-pressure minerals. *Phys. Earth Planet. Int.* **96**, 85–112 (1996).

25. Cahn, J. W., Shechtman, D. & Gratias, D. Indexing of icosahedral quasiperiodic crystals. *J. Mat. Res.* **1**, 13–26 (1986).

26. Nishihara, Y., Takahashi, E., Matsukage, K. & Kikegawa, T. Thermal equation of state of omphacite. *Am. Mineral.* **88**, 80–86 (2003).

27. Steurer, W. & Deloudi, S. *Crystallography of Quasicrystals. Concepts, Methods and Structures.* Springer, Berlin (2009).

28. Ponkratz, U., Nicula, R., Jianu, A. & Burkel, E. Quasicrystals under pressure: a comparison between Ti-Zr-Ni and Al-Cu-Fe icosahedral phases. *J. Non-Cryst. Sol.* **250–252**, 844–848 (1999).

29. Quivy, A. *et al.* High-resolution time-of-flight measurements of the lattice parameter and thermal expansion of the icosahedral phase $Al_{62}Cu_{25.5}Fe_{12.5}$. *J. Appl. Crystallogr.* **27**, 1010–1014 (1994).

30. Dobson, D. P. & Brodholt, J. P. The pressure medium as a solid-state oxygen buffer. *Geophys. Res. Lett.* **26**, 259–262 (1999).

31. Medard, E., McCammon, C. A., Barr, J. A. & Grove, T. L. Oxygen fugacity, temperature reproducibility, and H_2O contents of nominally anhydrous piston-cylinder experiments using graphite capsules. *Am. Mineral.* **93**, 1838–1844 (2008).

32. Rouxel, D. & Pigeat, P. Surface oxidation and thin film preparation of AlCuFe quasicrystals. *Progr. Surf. Sci.* **81**, 488–514 (2006).

33. Tsai, A. P. Discovery of stable icosahedral quasicrystals: progress in understanding structure and properties. *Chem. Soc. Rev.* **42**, 5352–5365 (2013).

34. Sadoc, A. *et al.* Quasicrystals under high pressure. *Physica B* **208**, 495 (1995).

35. Akahama, Y. *et al.* Pressure induced amorphization of quasicrystals. *J. Phys. Soc. Jap.* **58**, 2231–2234 (1989).

36. Bertka, C. M. & Fei, Y. Mineralogy of the Martian interior up to core-mantle boundary pressure. *J. Geophys. Res.* **102**, 5251–5264 (1997).

37. Lu, P. J., Deffeyes, K., Steinhardt, P. J. & Yao, N. Identifying and indexing icosahedral quasicrystals from powder diffraction patterns. *Phys. Rev. Lett.* **87**, 275507–1–275507–4 (2001).

38. Li, L., Bi, Q., Yang, J., Fu, L., Wang, L., Wang, S. & Liu, W. Large-scale synthesis of Al-Cu-Fe submicron quasicrystals. *Scripta Materialia* **59**, 587–590 (2008).

39. Oxford Diffraction. *CrysAlis RED* (Version 1.171.31.2) and *ABSPACK* in *CrysAlis RED*. Oxford Diffraction Ltd, Abingdon. Oxfordshire, England (2006).

40. Katsura, T. *et al.* A large-volume high-pressure and high-temperature apparatus for in situ X-ray observation, 'SPEED-Mk. II'. *Phys. Earth Planet. Int.* **143–144**, 497–506 (2004).

41. Tange, Y. *et al.* *P–V–T* equation of state of $MgSiO_3$ perovskite based on the MgO pressure scale: A comprehensive reference for mineralogy of the lower mantle. *J. Geophys. Res.* **117**, B06201 (2012).

42. Seto, Y., Hamane, D., Nagai, T. & Sata, N. Development of a software suite on X-ray diffraction experiments. *Rev. High Press. Sci. Tech.* **20**, 269–276 (2010).

Acknowledgments

Author contributions

All authors contributed equally to this work. The study was conceived and guided by V.S. and L.B. V.S., L.B., P.J.S., Y.F. and H.-K.M. designed the research. V.S. and Y.S. performed in situ diffraction experiment at Spring-8 with the technical support of Y.T and Y.H. V.S. performed additional quench experiments, chemical analyses and powder X-ray diffraction of the recovered run products. L.B. performed X-ray single crystal diffraction of both starting materials and quenched samples. All the authors discussed the results and commented on the manuscript.

Additional information